Acta Chemica Scandinavica, 1998: 52: 883–890
Printed in UK – all rights reserved

ACTA
CHEMICA SCANDINAVICA
ISSN 0904-213X

Crystal Structures and Luminescence Spectra of Transition Metal Complexes of Rhodamine 6G: $R_2[CuCl_4]\cdot 3H_2O$ and $R_2[MnCl_4]\cdot (EtOH)_{1/2}$ [R = 9-(2-Ethoxycarbonyl)phenyl-3,6-bis(ethylamino)-2,7-dimethylxanthylium]

Cai-Ming Liu,[a] Ren-Gen Xiong,[a] Xiao-Zeng You[a,*] and Wei Chen[b]

[a]Coordination Chemistry Institute, State Key Laboratory of Coordination Chemistry, Nanjing University, Center for Advance Studies in Science and Technology of Microstructure, Nanjing 210093, People's Republic of China and [b]Department of Chemistry, University of Malaya, Kuala Lumpur 59100, Malaysia

Liu, C.-M., Xiong, R.-G., You, X.-Z. and Chen, W., 1998. Crystal Structures and Luminescence Spectra of Transition Metal Complexes of Rhodamine 6G: $R_2[CuCl_4]\cdot 3H_2O$ and $R_2[MnCl_4]\cdot (EtOH)_{1/2}$ [R = 9-(2-Ethoxycarbonyl)-phenyl-3,6-bis(ethylamino)-2,7-dimethylxanthylium]. – Acta Chem. Scand. 52: 883–890. © Acta Chemica Scandinavica 1998.

Bis(9-(2-ethoxycarbonyl)phenyl-3,6-bis(ethylamino)-2,7-dimethylxanthylium) tetrachlorocopper(II) trihydrate solvate (**1**) was obtained by reaction of rhodamine 6G with $CuCl_2 6H_2O$ in the presence of hydrochloride under reflux for 1 h, the structure of which was determined by X-ray diffraction. The complex belongs to the monoclinic space group $C2/c$, with $a = 28.271(7)$, $b = 14.829(2)$, $c = 15.892(3)$ Å, $\beta = 117.29(1)°$, $V = 5921(2)$ Å^3, $Z = 4$, $R_1 = 0.0994$, $wR_2 = 0.2424$. The copper ion is located on crystallographic two-fold axis and has a coordination geometry intermediate between tetrahedral and square planar. There are hydrogen-bonding interactions among tetrachloro cuprate(2−) ions and rhodamine 6G cations, and π–π stacking interactions between rhodamine 6G cations. Another transition metal complex of rhodamine 6G bis(9-(2-ethoxycarbonyl)-phenyl-3,6-bis(ethylamino)-2,7-dimethylxanthylium) tetrachloro manganese(II) demiethanol solvate (**2**) was prepared by reflux of ethanol solution of rhodamine 6G and $MnCl_2 6H_2O$ for 1 h. This complex crystallizes in the triclinic space group P_1 with $a = 11.677(2)$, $b = 12.532(1)$, $c = 20.683(1)$ Å, $\alpha = 99.42(3)$, $\beta = 99.57(1)$, $\gamma = 96.46(2)$, $V = 2913.8(5)$, $Z = 2$, $R_1 = 0.0659$, $wR_2 = 0.1300$. The anion $MnCl_4^{2-}$ exhibits a very slightly distorted tetrahedron with Mn–Cl bond distances 2.355(1)–2.375(1) Å. All chlorine atoms in $MnCl_4^{2-}$ are hydrogen-bonded to the ethanol molecules and rhodamine 6G cations, and there are π–π stacking interactions between rhodamine 6G cations. Blue-shifts were observed in the solid state fluorescence of complex **1** and **2** with respect to rhodamine 6G. The larger blue-shift of complex **1** relative to that of complex **2** could be attributed to the packing effects. In addition, the IR spectra of two compounds are discussed and related to their structures.

Rhodamine 6G and its derivatives, with their excellent photophysical properties, have found applications in concentrators of solar diagnostic devices,[1] in electroluminescent devices,[2] in tunable lasers,[3] and in photographic[4] and fluorescence depolarization diagnostic devices.[5] Furthermore, they have been extensively used in medical science, biology and analytical chemistry.[6,7] Recently, the complexes of rhodamine 6G with a metal ion have also aroused considerable interest.[8–10] Previously, we reported the first crystal structure example of rhodamine 6G with cadmium ions, $R_2[CdCl_4]\cdot EtOH\cdot H_2O$.[11] Compared to the crystal structure of 9-[2-(ethoxycarbonyl)phenyl]-3,6-bis(ethylamino)-2,7-dimethylxanthylium iodide monohydrate $RI\cdot H_2O$,[12] the former was found to possess π–π stacking interaction, suggesting that the different anions have an influence on the aggregative properties of cations of rhodamine 6G. In this area, we here extend the research on complexes of rhodamine 6G with other metal ions. This paper reports the crystal structures of $R_2CuCl_4\cdot 3H_2O$ and $R_2MnCl_4\cdot (EtOH)_{1/2}$, and their luminescence spectra in the solid state.

* To whom correspondence should be addressed.

Experimental

Synthesis. Rhodamine 6G was obtained from E. Merck and was used without further purification.

$R_2CuCl_4 \cdot 3H_2O$ (**1**). To an ethanol solution of rhodamine 6G (2 mmol, 20 ml) was added an aqueous solution of $CuCl_2 \cdot 6H_2O$ (1 mmol, 5 ml) with stirring. Then an excess of concentrated hydrochloride was added dropwise during a reflux period. After 1 h, the solution was cooled to room temperature and left to evaporate for several weeks to give deep shiny green crystals, yield 90%. *Anal.* Found: C, 58.5; H, 6.1; N, 4.8. Calc. for $R_2CuCl_4 \cdot 3H_2O$: C, 58.67; H, 5.98; N, 4.98%.

$R_2MnCl_4 \cdot (EtOH)_{1/2}$ (**2**). 1 mmol $MnCl_2 \cdot 6H_2O$ was dissolved in 20 ml of ethanol, and then 20 ml of ethanol solution of rhodamine 6G(1 mmol) was added. The shiny red solution was refluxed for 1 h, whereafter brown red crystals were obtained by slow evaporation at room temperature for a few days, yield 75%. *Anal.* Found: C, 61.6; H, 3.0; N, 2.4; Calc. for $R_2MnCl_4 \cdot (EtOH)_{1/2}$: C, 61.85; H, 2.96; N, 2.53%.

Physical measurements. Elemental analyses for C, H and N were performed on a Perkin–Elmer 240 analyser. IR spectra were obtained with KBr pellets in the 4000–400 cm^{-1} region, using a Nicolet 170 SX-FTIR spectrophotometer. Luminescence spectra were recorded on a HITACHI 850 fluorescence spectrophotometer at room temperature (298 K).

X-Ray structure determination of $R_2CuCl_4 \cdot 3H_2O$ (**1**). A shiny violet–green, prismatic crystal was cleaved from a larger sample, selected for X-ray analysis and mounted on an Enraf–Nonius CAD4 diffractometer. Crystal data, collection and refinement details are listed in Table 1. A systematic search in a limited hemisphere of reciprocal space gave a set of diffraction maxima corresponding to a monoclinic space group, either *Cc* or *C2/c*. The structure was then solved by the direct method in space group *Cc*. The origin of the cell was later shifted to a center of inversion in a *C2/c* cell. Cell parameters were obtained by a least-squares fit of 25 reflections in the range 5–11°. Intensity data were measured using the ω scan technique. A total of 5355 reflections were collected, of which 5251 were independent ones [R(int) = 0.0601]. 2156 reflections observed with $I > 2\sigma(I)$ were used in the structure solution and refinement. Intensity ψ-scan data were corrected for Lorentz and polarization effects.

The structure was solved by the direct method using SHELXS86[13] and refined using SHELX93.[14] All non-hydrogen atoms except the disordered water molecules were refined anisotropically. Hydrogen atoms were positioned geometrically and refined with riding mode. Residual electron density peaks were scattered around the 1.5 disordered water molecules which were assigned occupancies 0.5, 0.33, 0.33 and 0.33. The refinement was based on F^2. With weights $w = 1/[\sigma^2(F_o^2) + (0.1481P)^2 + 0.0000P]$, $P = (F_o^2 + 2F_c^2)/3$, the final residuals were $R_1 = 0.0994$, $wR_2 = 0.2424$. The maximum shift/e.s.d. ratio after final refinement cycle is 0.002.

X-Ray structure determination of $R_2MnCl_4 \cdot (EtOH)_{1/2}$ (**2**). A shiny red, octahedral crystal was selected for X-ray analysis. The intensities were collected at 291(2) K on a Siemens P4 four-circle diffractometer with monochromated MoKα (λ = 0.71073 Å) radiation using θ/2θ scan mode with a variable scan speed 5.0–50.0° min^{-1} in ω. The data were corrected for Lorentz and polarization effects using XSCANS.[15] Details of crystal data, collection and refinement are listed in Table 1.

The structure was solved by the Patterson method and refined on F_o^2 by full-matrix least-squares methods using SHELXTL version 5.0[16] on a Pc-586. Analytical expressions of neutral-atom scattering factors were employed and anomalous dispersion corrections were incorporated.[17] All the non-hydrogen atoms were refined anisotropically. Hydrogen atoms were placed in calculated positions (C–H, 0.96; N–H, 0.90; and O–H, 0.85 Å) and assigned fixed isotropic thermal parameters at 1.2 times (1.5 times for methyl groups). The equivalent isotropic U factors of the atoms to which they are attached (1.5 times for the O–H and methyl groups) and allowed to ride on their respective parent atoms. The contributions of these hydrogen atoms were included in the structure-factor calculations.

Results and discussion

Atomic coordinates for the non-hydrogen atoms of complexes **1** and **2** are given in Tables 2 and 3. Relevant bond distances and angles are listed in Tables 4 and 5.

Crystal structure of $R_2CuCl_4 \cdot 3H_2O$ (**1**). The structure of complex **1** consists of discrete $CuCl_4^{2-}$ anions, rhodamine 6G cations and water molecules (Fig. 1). Like $R_2[CdCl_4] \cdot EtOH \cdot H_2O$,[11] complex **1** does not display a perovskite-type layer compound feature due to the lack of a primary ammonium cation, although such a structure was obtained under acidic conditions. To our knowledge, the perovskite-type layer compounds, with general formula $(C_nH_{2n+1}NH_3)_2MX_4$ (with $M = Cd^{2+}$, Mn^{2+}, Cu^{2+}, ..., X = Cl, Br), were obtained by mixing alcoholic solutions of *n*-alkylammonium chloride (prepared by HCl on the corresponding amine) and MX_2.[18] The crystalline structure of these compounds consists of alternating two-dimensional layers built up from corner-sharing MX_6 octahedra and aligned alkylammonium chains occupied between these layers. The NH_3 polar ends of the chains are linked to the chlorine matrix by hydrogen bonds, whereas the CH_3 ends of the chains are directed towards the interlayer space and are interacted each other through van der Walls forces.[18] The copper ion in complex **1** locates on a crystallographic two-fold axis and has a coordination geometry intermediate between tetrahedral and square planar. This geometry is very similar to that of $[C_5H_7N_2]_2[CuCl_4] \cdot H_2O$[19] and $[C_5H_7N_2O]_2[CuCl_4]$,[19] but different from that of

Table 1. Crystal data for $R_2CuCl_4 \cdot 3H_2O$ (**1**) and $R_2MnCl_4 \cdot (EtOH)_{1/2}$ (**2**), R = 9-(2-ethoxycarbonyl)phenyl-3,6-bis(ethylamino)-2,7-dimethylxanthylium.

Compound	**1**	**2**
Formula	$C_{56}H_{68}Cl_4CuN_4O_9$	$C_{57}H_{65}Cl_4MnN_4O_{6.5}$
Formula mass	1146.48	1106.87
Colour, Habit	Shiny green, prism	Shiny red, octahedraon
Crystal system	Monoclinic	Triclinic
Space group	$C2/c$	$P\bar{1}$
Wavelength/Å	0.71073	0.71073
Temperature/K	300(2)	291(2)
a/Å	28.271(7)	11.677(2)
b/Å	14.829(2)	12.532(1)
c/Å	15.892(3)	20.683(1)
α/°	90.00	99.42(3)
β/°	117.29(1)	99.57(1)
γ/°	90.00	96.46(2)
V/Å^3	5921(2)	2913.8(5)
Z	2	2
D_c/g cm^{-3}	1.286	1.262
Crystal size/mm	0.3 × 0.25 × 0.2	0.35 × 0.42 × 0.53
F(000)	2404	1160
μ/mm^{-1}	0.605	0.461
2θ min, max/°	3.18, 50.20	3.56, 45.00
No. of reflections collected	5355	8980
No. of independent reflections	5251 [R(int) = 0.0601]	7621[R(int) = 0.0393]
Data/restraints/parameters	5251/0/338	7608/0/668
Goodness-of-fit on F^2	0.931	1.084
Final R-indices [$I > 2\sigma(I)$]	$R_1 = 0.0994$, $wR_2 = 0.2424$	$R_1 = 0.0659$, $wR_2 = 0.1300$
R-indices (all data)	$R_1 = 0.1958$, $wR_2 = 0.2923$	$R_1 = 0.1603$, $wR_2 = 0.1724$
Largest difference peak and hole (e Å^{-3})	0.831 and −0.339	0.470 and −0.299

Agreement factors are refined as follows: $R_1 = \Sigma||F_o| - |F_c||/\Sigma|F_o|$, $wR_2 = \{\Sigma[w(F_o^2 - F_c^2)^2]/\Sigma[w(F_o^2)^2]\}^{1/2}$ and $S = [\Sigma[w(F_o^2 - F_c^2)^2]/(n-P)]^{1/2}$ for both complexes.

$[C_5H_8N_2]_2[CuCl_4] \cdot H_2O$,[20] $[C_8H_{20}N_2O_2]_2[CuCl_4]$[20] and $[H_3NC_4H_8NH_3][CuCl_4]$.[21] The latter three compounds consist of two-dimensional perovskite-type $[CuCl_4^{2-}]_n$ layers. The *trans* bond angles are both 136.20(11)° for Cl(1)^i–Cu–Cl(2) and Cl(1)–Cu–Cl(2)^i (the symmetry operation^i is $-X, Y, -Z+1/2$), which are comparable to those of $[C_5H_7N_2]_2[CuCl_4] \cdot H_2O$ [134.6(1)°][19] and $[C_5H_7N_2O]_2[CuCl_4]$ [137.9(1)°].[19] The Cu–Cl(2) bond and Cu–Cl(2)^i bond [both are 2.254(3) Å] are longer than the Cu–Cl(1) bond and Cu–Cl(1)^i [both are 2.231(3) Å] due to their extensive involvement in hydrogen-bonding. The Cl(2) atom is hydrogen-bonded to N(1) and N(2) of different rhodamine 6G cations, with the hydrogen bond lengths [Cl(2)···N(1)^{ii} 2.372(14) Å, ^{ii} is $1/2+X, 1/2+Y, Z$ and Cl(2)···N(2) 3.460(14) Å].

The xanthene ring of the cation is planar with the phenyl ring tilted at an angle of 77.5(3)° due to sterical hindrance. The tilting is a little smaller than that in $RI \cdot H_2O$ [79.75(15)°],[12] partly owing to the particular arrangement of the carbonyl ring. There are two inverse possibilities for the arrangement of the carbonyl group. Previous theory has suggested that the most probable configuration of the rhodamine 6G cation is when the carbonyl group is situated near the xanthene ring,[22] and the crystal structures of $RI \cdot H_2O$[12] and $R_2[CdCl_4] \cdot EtOH \cdot H_2O$[11] have confirmed the existence of this configuration. However, complex **1** adopts the inverse configuration in which the carbonyl group in $-CO_2C_2H_5$ is far away rather than near to the xanthene ring, with the C(12)–C(13)–O(3)–C(14) torsional angle being −179.8(8)°. The torsional angles for C(3)–N(1)–C(4)–C(5) are −83(1)° and for C(24)–N(2)–C(25)–C(26) −155(1)°.

The C–N bond distances of N(1)–C(4) and N(2)–C(25) are 1.427(11) and 1.483(13) Å, indicating normal C–N single bonds, respectively, whereas C(3)–N(1) and C(24)–N(2) are much shorter [1.342(10) and 1.345(10) Å, respectively], showing partial double-bond character. This indicates that the cation has delocalized bonding election. Similar trends have also been observed in $R_2[CdCl_4] \cdot EtOH \cdot H_2O$[11] and $RI \cdot H_2O$.[12] The C–O and C–C bond lengths are comparable to those in $R_2[CdCl_4] \cdot EtOH \cdot H_2O$[11] and $RI \cdot H_2O$.[12]

As shown in Fig. 2, the $CuCl_4^{2-}$ anions form layers normal to the a-direction separated by layers of rhodamine 6G cations. The xanthene rings form stacks running in the (103) and (10$\bar{3}$) directions. The anionic and cationic layers are held together by the N–H···Cl hydrogen bonds as discussed above. Furthermore, the distance between two xanthene planes is about 3.5–3.6 Å [O(1)···C(1)^{iii} 3.645(13), C(10)···H(2a)^{iii} 3.548(13), N(2)···H(7c)^{iii} 3.508(13); ^{iii} is $-1/2-X, -1/2-Y, 1-Z$), indicative of significant π–π stacking interaction between two neighbour rhodamine 6G cations whose carbonyl groups are arranged in the opposite directions.

Table 2. Atomic coordinates (in Å) and equivalent isotropic displacement parameters (in Å^2) for complex **1**.

Atom	*x/a*	*y/b*	*z/c*	$U_{iso/eq}$[a]
Cu	0.0000	−0.1357(1)	0.2500	0.053(1)
Cl(1)	0.0645(1)	−0.2344(2)	0.3316(3)	0.097(1)
Cl(2)	0.0167(1)	−0.0343(2)	0.3659(2)	0.059(1)
O(1)	−0.2149(2)	−0.2989(4)	0.4168(4)	0.042(1)
O(2)	−0.3138(4)	−0.0448(6)	0.0718(6)	0.120(3)
O(3)	−0.3162(3)	−0.1646(5)	0.1493(4)	0.069(2)
N(1)	−0.3648(3)	−0.4664(5)	0.3855(5)	0.049(2)
N(2)	−0.0591(3)	−0.1563(5)	0.4459(5)	0.057(2)
C(1)	−0.2684(3)	−0.3015(6)	0.3892(6)	0.037(2)
C(2)	−0.2887(3)	−0.3816(5)	0.4006(5)	0.039(2)
C(3)	−0.3435(3)	−0.3894(6)	0.3740(6)	0.041(2)
C(4)	−0.3357(4)	−0.5459(6)	0.4304(7)	0.056(3)
C(5)	−0.3242(5)	−0.6013(7)	0.3637(8)	0.080(3)
C(6)	−0.3773(3)	−0.3120(6)	0.3336(6)	0.039(2)
C(7)	−0.4354(3)	−0.3197(7)	0.3042(7)	0.060(3)
C(8)	−0.3558(3)	−0.2344(6)	0.3235(6)	0.040(2)
C(9)	−0.3004(3)	−0.2237(6)	0.3499(5)	0.038(2)
C(10)	−0.2771(3)	−0.1442(5)	0.3382(5)	0.034(2)
C(11)	−0.3088(3)	−0.0605(5)	0.3004(6)	0.038(2)
C(12)	−0.3261(3)	−0.0291(6)	0.2090(6)	0.047(2)
C(13)	−0.3182(4)	−0.0775(7)	0.1359(7)	0.057(3)
C(14)	−0.3084(5)	−0.2248(8)	0.0845(7)	0.084(4)
C(15)	−0.2708(6)	−0.3003(9)	0.1402(10)	0.118(5)
C(16)	−0.3529(4)	0.0525(7)	0.1826(7)	0.068(3)
C(17)	−0.3648(4)	0.1000(6)	0.2453(8)	0.070(3)
C(18)	−0.3483(4)	0.0680(7)	0.3345(7)	0.062(3)
C(19)	−0.3207(3)	−0.0119(6)	0.3625(6)	0.049(2)
C(20)	−0.2224(3)	−0.1441(5)	0.3641(5)	0.036(2)
C(21)	−0.1947(3)	−0.0697(6)	0.3546(5)	0.039(2)
C(22)	−0.1412(3)	−0.0713(5)	0.3819(5)	0.038(2)
C(23)	−0.1121(3)	0.0105(6)	0.3713(7)	0.058(3)
C(24)	−0.1114(3)	−0.1522(6)	0.4203(6)	0.042(2)
C(25)	−0.0256(4)	−0.2382(8)	0.4824(10)	0.095(4)
C(26)	0.0300(4)	−0.2183(8)	0.5401(9)	0.096(4)
C(27)	−0.1379(3)	−0.2274(6)	0.4331(6)	0.040(2)
C(28)	−0.1924(3)	−0.2223(5)	0.4035(6)	0.038(2)
O	−0.5000	0.0033(6)	0.2500	0.087(3)
O′	−0.4892(10)	0.0899(18)	0.3391(19)	0.104(8)
O″	−0.4422(10)	−0.0783(18)	0.3964(18)	0.102(8)
O‴	−0.4988(16)	−0.090(3)	0.335(3)	0.169(14)

[a] $U_{iso/eq}$ is defined as one third of the trace of the orthogonalized U_{ij} tensor.

Crystal structure of $R_2MnCl_4 \cdot (EtOH)_{1/2}$ (**2**). The structure of complex **2** consists of discrete $MnCl_4^{2-}$ anions, rhodamine 6G cations and ethanol molecules. Like $CdCl_4^{2-}$ in $[R_2CdCl_4] \cdot EtOH \cdot H_2O$,[11] the manganese atom is coordinated by chlorine atoms to form a very slightly distorted tetrahedron (Fig. 3), which is very similar to that of bis[benzyldimethyl(phenyl)ammonium]-tetrachloromanganate(II)[23] and $[N(CH_3)_4]_2MnCl_4$,[24] but quite different from that of $NH_3(CH_2)_4NH_3$-$MnCl_4$.[25] The $MnCl_4^{2-}$ in the latter form two-dimensional sheets of puckered perovskite-type layers of corner-sharing $MnCl_6$ octahedron, interleaved by layers of 1,4-butyldiammonium chains nearly perpendicular to the layers. However, like for $[R_2CdCl_4] \cdot EtOH \cdot H_2O$ [11] and $R_2CuCl_4 \cdot 3H_2O$ (**1**), the $[R_2MnCl_4]$ complex does not show a perovskite-type layer compound feature. The Mn–Cl bond lengths [2.355(1)–2.375(1) Å] are com-

Table 3. Atomic coordinates and equivalent isotropic displacement parameters for **2**.

Atom	*x/a*	*y/b*	*z/c*	$U_{iso/eq}$[a]
Mn(1)	0.8644(1)	0.5050(1)	0.2721(1)	0.052(1)
Cl(1)	0.6634(1)	0.4391(1)	0.2588(1)	0.092(1)
Cl(2)	0.9750(1)	0.4836(1)	0.3752(1)	0.050(1)
Cl(3)	0.9355(1)	0.4055(1)	0.1835(1)	0.074(1)
Cl(4)	0.8864(1)	0.6936(1)	0.2700(1)	0.102(1)
O(1)	0.5232(2)	−0.0523(1)	0.3872(1)	0.041(1)
O(2)	0.2820(2)	0.1279(2)	0.3143(1)	0.092(1)
O(3)	0.2143(2)	0.2833(2)	0.3078(1)	0.095(1)
N(1)	0.2349(2)	−0.3482(2)	0.3847(1)	0.053(1)
N(2)	0.8220(2)	0.2264(2)	0.3732(1)	0.061(1)
C(1)	0.2383(2)	−0.0570(2)	0.4425(1)	0.038(1)
C(2)	0.2013(2)	−0.1665(2)	0.4306(1)	0.038(1)
C(3)	0.2740(2)	−0.2402(2)	0.4012(1)	0.040(1)
C(4)	0.3826(2)	−0.1979(2)	0.3881(1)	0.041(1)
C(4A)	0.4166(2)	−0.0870(2)	0.4025(1)	0.036(1)
C(5)	0.6722(2)	0.0848(2)	0.3823(1)	0.042(1)
C(5A)	0.5653(2)	0.0584(2)	0.3991(1)	0.037(1)
C(6)	0.7192(2)	0.1952(2)	0.3919(1)	0.043(1)
C(7)	0.6560(2)	0.2766(2)	0.4205(1)	0.042(1)
C(8)	0.5502(2)	0.2462(2)	0.4355(1)	0.042(1)
C(8A)	0.4981(2)	0.1335(2)	0.4254(1)	0.034(1)
C(9)	0.3850(2)	0.1007(2)	0.4383(1)	0.036(1)
C(9A)	0.3469(2)	−0.0122(2)	0.4290(1)	0.033(1)
C(10)	0.2930(3)	−0.4300(2)	0.3489(1)	0.062(1)
C(11)	0.3944(3)	−0.4661(2)	0.3922(2)	0.076(1)
C(12)	0.0840(2)	−0.2097(2)	0.4448(1)	0.053(1)
C(13)	0.8871(3)	0.1580(2)	0.3329(2)	0.097(2)
C(14)	0.9526(4)	0.0849(3)	0.3706(2)	0.146(2)
C(15)	0.7080(3)	0.3967(2)	0.4364(1)	0.061(1)
C(16)	0.2503(2)	0.2378(2)	0.4143(1)	0.045(1)
C(17)	0.1835(2)	0.3157(2)	0.4368(1)	0.055(1)
C(18)	0.1735(3)	0.3351(2)	0.5026(2)	0.064(1)
C(19)	0.2318(3)	0.2788(2)	0.5476(1)	0.060(1)
C(20)	0.2986(2)	0.2039(2)	0.5254(1)	0.052(1)
C(21)	0.3099(2)	0.1813(2)	0.4596(1)	0.038(1)
C(22)	0.2533(3)	0.2098(2)	0.3413(2)	0.057(1)
C(23)	0.2050(4)	0.2616(3)	0.2340(2)	0.119(2)
C(24)	0.2839(5)	0.3322(4)	0.2109(2)	0.186(3)
O(4)	0.9557(2)	0.8553(1)	−0.0490(1)	0.052(1)
O(5)	1.2870(2)	0.9751(2)	0.0739(1)	0.079(1)
O(6)	1.4730(2)	0.9829(2)	0.1226(1)	0.089(1)
N(3)	0.8866(2)	0.5921(2)	0.0844(1)	0.062(1)
N(4)	0.9914(2)	1.1126(2)	−0.1893(1)	0.060(1)
C(31)	1.1550(3)	0.6893(2)	0.0320(1)	0.047(1)
C(32)	1.0828(2)	0.6311(2)	0.0620(1)	0.047(1)
C(33)	0.9617(3)	0.6476(2)	0.0542(1)	0.048(1)
C(34)	0.9237(3)	0.7271(2)	0.0169(1)	0.051(1)
C(34A)	1.0016(2)	0.7820(2)	−0.0121(1)	0.043(1)
C(35)	0.9720(3)	0.9840(2)	−0.1171(1)	0.049(1)
C(35A)	1.0262(2)	0.9137(2)	−0.0813(1)	0.044(1)
C(36)	1.0415(3)	1.0441(2)	−0.1526(1)	0.049(1)
C(37)	1.1620(2)	1.0343(2)	−0.1513(1)	0.045(1)
C(38)	1.2104(2)	0.9638(2)	−0.1144(1)	0.043(1)
C(38A)	1.1450(2)	0.8996(2)	−0.0781(1)	0.044(1)
C(39)	1.1919(2)	0.8272(2)	−0.0379(1)	0.038(1)
C(39A)	1.1184(2)	0.7676(2)	−0.064(1)	0.040(1)
C(40)	0.7664(3)	0.6064(3)	0.0855(2)	0.081(1)
C(41)	0.6819(3)	0.5430(3)	0.0294(2)	0.107(2)
C(42)	1.1265(3)	0.5509(2)	0.1028(1)	0.064(1)
C(43)	0.8658(3)	1.1225(2)	−0.1980(2)	0.083(1)
C(44)	0.8284(4)	1.1808(3)	−0.2482(2)	0.152(2)
C(45)	1.2322(3)	1.0967(2)	−0.1901(1)	0.061(1)
C(46)	1.4084(2)	0.8658(2)	0.0184(1)	0.041(1)
C(47)	1.5227(3)	0.8469(2)	0.0173(1)	0.055(1)
C(48)	1.5496(3)	0.7769(2)	−0.0334(1)	0.061(1)

Table 3. (Continued.)

C(49)	1.4620(3)	0.7224(2)	−0.0856(1)	0.064(1)
C(50)	1.3475(3)	0.7408(2)	−0.0853(1)	0.053(1)
C(51)	1.3193(2)	0.8127(2)	−0.0345(1)	0.041(1)
C(52)	1.3821(3)	0.9451(2)	0.0741(1)	0.057(1)
C(53)	1.4448(4)	1.0560(3)	0.1803(2)	0.159(2)
C(54)	1.5395(4)	1.1092(3)	0.2216(2)	0.163(2)
O(7)	0.5354(3)	0.6584(3)	0.2838(2)	0.081(2)
C(56)	0.5417(6)	0.7012(5)	0.2337(4)	0.127(3)
C(55)	0.4744(6)	0.6662(7)	0.1804(4)	0.137(4)

[a] $U_{iso/eq}$ is defined as in Table 2.

parable to those in $[N(CH_3)_4]_2MnCl_4$ [2.309(13)–2.369(16), 2.329(3)–2.360(8), 2.345(4)–2.351(30) and 2.356(5)–2.372(13) Å][24] but much shorter than those in $NH_3(CH_2)_4NH_3MnCl_4$ [2.502(4)–2.608(5) Å].[25] The Cl–Mn–Cl bond angles fall in the range 107.03(4)–112.95(4)°, which is very similar to those in $[N(CH_3)_4]_2MnCl_4$ [105.6(7)–112.4(7), 106.7(3)–112.3(14), 106.9(9)–112.3(2) and 106.7(13)–112.4(3)°].[24]

Both xanthene rings of the cations are planar. The dihedral angle between the phenyl ring [C(16)C(17)C(18)C(19)C(20)C(21)] and the xanthene plane is 76.2(3)° and smaller than that between the phenyl ring [C(46)C(47)C(48)C(49)C(50)C(51)] and the xanthene plane [83.9(3)°]. Unlike in complex **1**, two rhodamine 6G cations in complex **2** adopt normal configuration where the carbonyl group is situated near the xanthene ring as those in $R_2[CdCl_4]\cdot EtOH\cdot H_2O$[11] and $RI\cdot H_2O$.[12] The torsional angles are −112.2(3)° for C(22)–O(3)–C(23)–C(24) and −167.5(3)° for C(52)–O(6)–C(53)–C(54). Furthermore, the torsional angles involving N atoms of two rhodamine 6G cations are also different; in the rhodamine 6G cation containing the O(1) atom, the torsional angles are 80.2(3)° for C(3)–N(1)–C(10)–C(11) and 76.3(3)°for C(6)–N(2)–C(13)–C(14) in the other rhodamine 6G cation [containing the O(4) atom], they are 87.0(3)° for C(33)–N(3)–C(40)–C(41) and −167.8(3)° for C(36)–N(4)–C(43)–C(44).

In the rhodamine 6G cation containing the O(1) atom, the C–N bond distances of N(1)–C(10) and N(2)–C(13) are 1.461(4) and 1.460(4) Å, respectively, belonging to the normal kind of C–N single bonds, whereas C(3)–N(1) and C(6)–N(2) are much shorter [1.347(3) and 1.358(4) Å, respectively] showing partial double-bond character. A similar trend is observed in the other rhodamine 6G cation: the C–N bond distances of N(3)–C(40) and N(4)–C(43) are 1.438(4) and 1.468(4) Å, whereas much shorter C(33)–N(3) and C(36)–N(4)

Table 4. Selected bond distances (in Å) and angles (in °) for complex **1**.

Cu–Cl(1)^i	2.231(3)	Cu–Cl(1)	2.231(3)
Cu–Cl(2)	2.254(3)	Cu–Cl(2)^i	2.254(3)
N(1)–C(3)	1.342(10)	N(1)–C(4)	1.427(11)
N(2)–C(24)	1.345(10)	N(2)–C(25)	1.483(13)
O(1)–C(28)	1.365(9)	O(1)–C(1)	1.368(8)
O(2)–C(13)	1.184(11)	O(3)–C(13)	1.307(11)
O(3)–C(14)	1.454(12)	C(10)–C(11)	1.486(10)
Cl(1)^i–Cu–Cl(1)	98.0(2)	Cl(1)^i–Cu–Cl(2)	136.20(11)
Cl(1)–Cu–Cl(2)	98.85(11)	Cl(1)^i–Cu–Cl(2)^i	98.85(11)
Cl(1)–Cu–Cl(2)^i	136.20(11)	Cl(2)–Cu–Cl(2)^i	96.27(14)
C(1)–O(1)–C(28)	119.9(6)	C1(3)–O(3)–C(14)	120.0(9)
C(3)–N(1)–C(4)	125.4(7)	C(24)–N(2)–C(25)	124.8(8)

Symmetry code: ^{i} $-X, Y, -Z+1/2$.

Table 5. Selected bond distances (in Å) and angles (in °) for complex **2**.

Mn(1)–Cl(1)	2.355(1)	Mn(1)–Cl(4)	2.357(1)
Mn(1)–Cl(3)	2.364(1)	Mn(1)–Cl(2)	2.375(1)
O(1)–C(4A)	1.376(3)	O(1)–C(5A)	1.386(3)
O(2)–C(22)	1.195(3)	O(3)–C(22)	1.317(4)
O(3)–C(23)	1.490(4)	N(1)–C(3)	1.347(3)
N(1)–C(10)	1.461(4)	N(2)–C(6)	1.358(4)
N(2)–C(13)	1.460(4)	O(4)–C(34A)	1.385(3)
O(4)–C(35A)	1.366(3)	O(5)–C(52)	1.210(4)
C(9)–C(21)	1.472(4)	C(39)–C(51)	1.510(4)
Cl(1)–Mn(1)–Cl(4)	108.93(5)	Cl(1)–Mn(1)–Cl(3)	107.19(4)
Cl(4)–Mn(1)–Cl(3)	111.68(4)	Cl(1)–Mn(1)–Cl(2)	112.95(4)
Cl(4)–Mn(1)–Cl(2)	107.03(4)	Cl(3)–Mn(1)–Cl(2)	109.13(4)
C(4A)–O(1)–C(5A)	119.8(2)	C(22)–O(3)–C(23)	118.2(2)
C(3)–N(1)–C(10)	125.5(2)	C(6)–N(2)–C(13)	127.1(2)
C(52)–O(6)–C(53)	113.8(3)	C(33)–N(3)–C(40)	126.6(3)
C(36)–N(4)–C(43)	123.2(3)	C(34A)–O(4)–C(35A)	119.6(2)

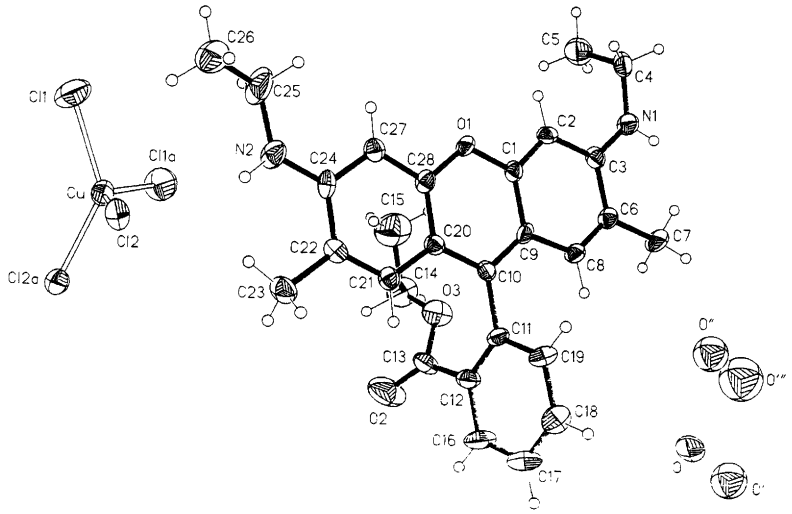

Fig. 1. Molecular structure of complex **1**.

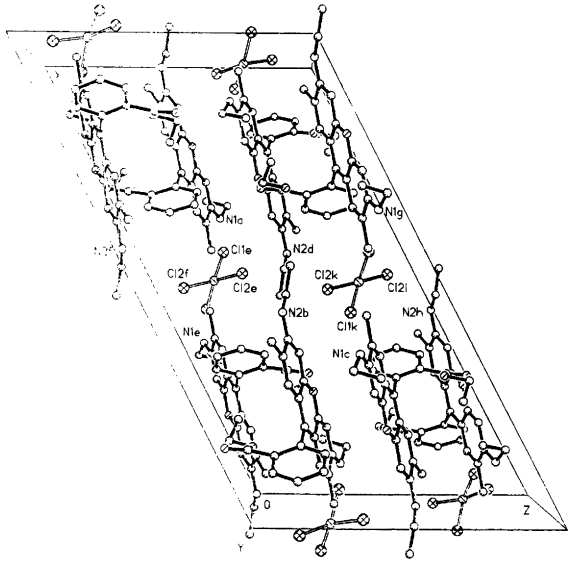

Fig. 2. Unit-cell packing diagram of complex **1**.

distances [1.353(4) and 1.354(4) Å, respectively] also display the partial double-bond character. This indicates that both rhodamine 6G cations have delocalized electron clouds.

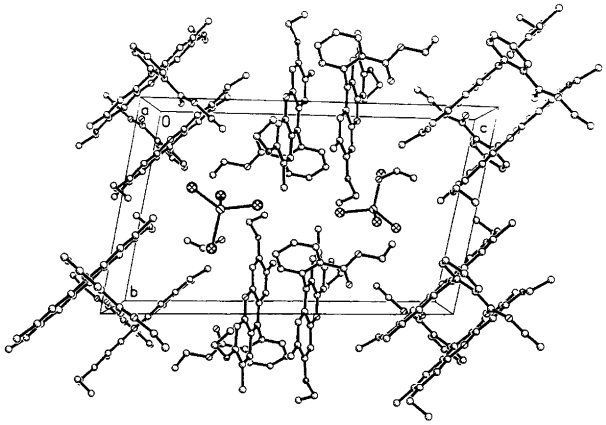

Fig. 4. Unit-cell packing diagram of complex **2**.

The crystal lattice is stabilized by not only electrostatic interactions but also hydrogen-bonding interactions. All chlorine atoms in $MnCl_4^{2-}$ are involved in hydrogen-bonding. In detail, Cl(2) is hydrogen-bonded to N(1) and N(2) of different rhodamine 6G cations [N(2)···Cl(2), 3.495(5) Å, N(1)*···Cl(2), 3.452(5) Å, * is $-1+X, -1+Y, Z$), Cl(3) and Cl(4) are hydrogen-bonded to N(3) of one rhodamine 6G cation

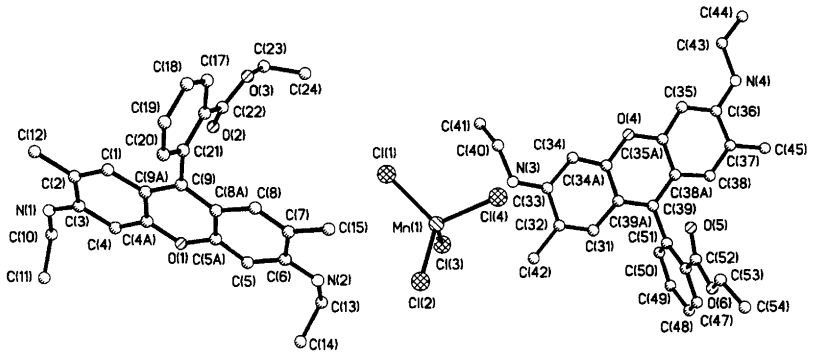

Fig. 3. Molecular structure of complex **2**.

[N(3)···Cl(3), 3.388(5) Å] and N(4) of another rhodamine 6G cation [N(4)–Cl(4)^{iv}, 3.473(4) Å, ^{iv} is $2-X, 2-Y, -Z$), respectively, while Cl(1) is connected to an ethanol molecule with a hydrogen bond [O(7)···Cl(1), 3.282(4) Å]. Furthermore, there exist π–π stacking interactions between rhodamine 6G cations which also stabilize the crystal lattice. The distances between two xanthene planes are 3.63(3) Å [with a center-to-center distance of 3.771(6) Å] for the two rhodamine 6G cations containing O(1) and O(1)^{v} (^{v} is $1-X, -Y, 1-Z$) respectively, and 3.54(3) Å [with a center-to-center distance of 4.686(8) Å] for the two rhodamine 6G cations containing O(4) and O(4)^{vi} (^{vi} is $2-X, 2-Y, -Z$), respectively. Every pair of rhodamine 6G cations involving π–π stacking interactions are arranged with their carbonyl groups in the opposite directions as suggested in complex **1**.

IR spectra and luminescence spectra in solid state. The IR spectrum of the complex **1** shows a large strong absorption band at 3301 cm^{-1} belonging to the O–H stretching vibration of non-coordinated water. Another strong absorption band at 1607 cm^{-1} is also assigned to water. The strong absorption bands at 1717 and 1308 cm^{-1} are attributed to the C=O and C–O stretching modes, respectively. In the IR spectrum of the complex **2**, the absorption band at 3438 cm^{-1} is attributed to the O–H stretching mode of ethanol, while two large absorption bands at 3321 and 3281 cm^{-1} are assigned to the N–H stretching modes of ammonium. Two strong absorption bands at 1712 and 1308 cm^{-1} are again attributed to C=O and C–O stretching modes. It should be noted that the C=O stretching vibration of complex **1** occurs at higher wavenumbers than that of complex **2**, reflecting the quite different structural arrangements of carbonyl group in both complexes.

The luminescence spectra were obtained for the powdered solid at room temperature with $\lambda_{ex}=433.4$ nm. A small blue-shift of 15 nm was observed in the spectrum of complex **2** (652 nm) compared to that of rhodamine 6G (667 nm). The spectral difference may mainly originate from the influence of the anions. There is an electrostatic interaction between the anion and the positively charged nitrogen in the rhodamine 6G cation. This interaction compensates the positive charge on the nitrogen, and restricts its oscillatory behavior as previously suggested.[26] Since the $MnCl_4^{2-}$ anion is larger and more reductive than the Cl^- anion in rhodamine 6G, the electrostatic interaction within complex **2** is more remarkable than that of rhodamine 6G, therefore a spectral shift to higher energy is expected. The electrostatic interaction between $CuCl_4^{2-}$ and rhodamine 6G cations in complex **1** is comparable to that between $MnCl_4^{2-}$ and rhodamine 6G cations in complex **2.** However, a large blue-shift (53 nm) was observed in the spectra of complex **1** (614 nm) with respect to the rhodamine 6G (667 nm). The packing effects should be taken into account in order to explain why the blue-shift of complex **1** is larger than that of complex **2**, since earlier research has indicated that there is a relation between the packing effects and solid state fluorescence of dyes.[27] The presence of $-CO_2C_2H_5$ of adopting abnormal configuration in complex **1** (i.e. the carbonyl group in $-CO_2C_2H_5$ is far away the xanthene ring) favors the tight aggregation of the rhodamine 6G cations. In complex **1,** all xanthene rings of rhodamine 6G cations are arranged in parallel planes (along the 103 direction). Each pair of rings are almost back to back and involve π–π stacking interaction. However, in complex **2**, the carbonyl group adopts normal configuration (it is near to the xanthene ring), and the two xanthene rings of rhodamine 6G cations are arranged in two directions (i.e. 010 and 012 directions), so that the π–π stacking interactions are not so intense as in complex **1** [as the larger center-to-center distance 4.686(8) Å of two xanthene planes in complex **2** suggests], and a larger blue-shift of complex **1** is expected.

Acknowledgments. This work was supported by a grant for a key research project from the State Science and Technology Commission, the National Nature Science Foundation of China, as well as the Foundation of the Chinese Postdoctoral Fellowship and the Fund of University of Malaya (IRPA Grant no. 09-02-03-0004).

References

1. Weber, W. H. and Lambe, J. *Appl. Opt. 15* (1976) 2299; Batchelder, J. S., Zewail, A. H. and Cole, T. *Appl. Opt. 18* (1979) 3090; Bhownik, B. B., Chaud Huri, R. and Rohatgi-Mukherjee, K. K. *Ind. J. Chem., Sect. A 26* (1987) 95.
2. Johnson, G. E. and McGrane, K. M. *Proc. SPIE-Int. Soc. Opt. Eng. 1910* (1993) 6
3. Peterson, O. G., Tuccio S. A. and Snavely, B. B. *Appl. Phys. Lett. 17* (1970) 245; Yuzhakov, V. I. *Russ. Chem. Rev. 48* (1979) 1076; Nguyen D. H. and Meyer, Y. H. *Appl. Phys. B. 55* (1992) 409; Wittmann, M., Penzkofer, A. and Baeumler, W. *Opt. Commun. 90* (1992) 1982.
4. Norland, K., Ames, A. and Taylor, T. *Photogr. Sci. Eng. 14* (1970) 295.
5. Herz, A. H. *Photogr. Sci. Eng., 18* (1974) 223.
6. Neurath, A. R., Strick, N., Haberfield, P. and Jiang, S. *US Patent* 5 230 998 (1993).
7. Schuiling M. and Foerstel-Neuhaus, A. *Z. Pflanzenkr. Pflanzenschutz 99* (1992) 614.
8. Shimai, Y. and Katayama, T. *Jpn. KoKai, Tokkyo koho, Jpn. Patent* 03 267 140 (1991).
9. Bhagavthy, V., Reddy, M. L. P., Rao T. R. and Damodaran, A. D. *Ind. J. Chem., Sect. A 32* (1993) 463.
10. Wang, G., He, Y., Zhao, Z., Zhao, J. and Wang, F. *Yankuang Ceshi 12* (1993) 159.
11. Wang, H., Xiong, R.-G., Liu, C.-M., Chen, H.-Y., You, X.-Z. and Chen, W. *Inorg. Chim. Acta 254* (1997) 183.
12. Fun, H.-K., Chinnakali, K., Sivakumar, K., Liu, C.-M., Xiong, R.-G. and You, X.-Z. *Acta Crystallogr., Sect. C 53* (1997) 617.
13. Kopfman G. and Huler, R. *Acta Crystallogr., Sect. B 24* (1968) 348; Sheldrick, G. M. *Acta Crystallogr., Sect A 46* (1990) 467.
14. Sheldrick, G. M. *SHELXL 93, Program for Crystal Structure Refinement*, University of Göttingen, Germany 1993.
15. Siemens, *XSCANS (Version 2.1)*, Siemens Analytical X-ray Instruments Inc. Madison, WI 1994.

16. Siemens, *SHELXTL (Version 5.0)*, Siemens Industrial Automation, Inc. Analytical Instrumentation, Madison, WI 1995.
17. Wilson, A. J. C., Ed. *International Tables for X-Ray Crystallography*, Vol. C, Kluwer Academic Publishers, Dordrecht 1992. Tables 6.1.1.4 (pp. 500–502), 4.2.6.8 (pp. 219–22) and 4.2.42 (pp. 193–199), respectively.
18. Mokhlisse, R., Couzi, M., Chanh, N. B., Haget, Y., Hauw, C. and Meresse, A. *J. Phys. Chem. Solids. 46* (1985) 187 and references therein; Chanh, N. B., Hauw, C., Meresse, A., Rey-Lafon, M. and Ricard, L. A. *J. Phys. Chem. Solids 46* (1985) 1413 and references therein.
19. Halvorson, K. E., Patterson C. and Willett, R. D. *Acta Crystallogr., Sect. B 46* (1990) 508.
20. Willett, R., Place, H. and Middleton, M. *J. Am. Chem. Soc. 110* (1988) 8639.
21. Garland, J. K., Emerson, K. and Pressprich, M. R. *Acta Crystallogr., Sect. C 46* (1990) 1603.
22. Tamulis, A., Bazan, L. and Undzenas, A. *Spec. Publ. R. Soc. Chem. 91* (1991) 267.
23. Chaudhuri, S., Banerjee, T., Roy, P. N., Bocelli, G. and Deb Purkayasth, M. K. *Acta Crystallogr., Sect. C 46* (1990) 385.
24. Mashiyama,H. and Koshiji, N. *Acta Crystallogr., Sect. B 45* (1989) 467.
25. Tichy, K. Benes, J., Kind, R. and Arend, H. *Acta Crystallogr., Sect B 36* (1980) 1355.
26. López Arbeloa I. and Rohatgi-Mukherjee, K. K. *Chem. Phys. Lett. 128* (1986) 474; *129* (1986) 607.
27. Langhals, H., Demmig, S. and Potrawa, T. *J. Prakt. Chem. 333* (1991) 733.

Received October 28, 1997.